Sum Frequency Generation of Water on NaCl, $NaNO_3$, $KHSO_4$, HCl, HNO_3, and H_2SO_4 Aqueous Solutions

Cheryl Schnitzer, Steve Baldelli,† and Mary Jane Shultz*

Department of Chemistry, Tufts University, Medford, Massachusetts 02155

Received: June 29, 1999; In Final Form: October 29, 1999

The vapor−liquid interface of aqueous inorganic acid and salt solutions are examined using sum frequency generation (SFG). The results show that the SFG intensity of hydrogen-bonded water on 0.01*x* acid (HCl, HNO_3, and H_2SO_4) solutions, where x = mole fraction, is greatly enhanced compared to the 0.01*x* solution of the corresponding salts (NaCl, $NaNO_3$, and $KHSO_4$). This suggests that either surface water molecules on the acid solutions orient with the dipole in a more vertically aligned fashion than those on the salt solutions or that more layers of water are ordered. These results are interpreted with an electric double layer model, in which the double layer is composed of subsurface anions and cations. The weak association of protons, as opposed to Na^+ or K^+, with anions results in a greater electric field at the surface on acid solutions. The perturbation of surface water on ionic solutions is discussed in terms of electrostatic and displacement mechanisms.

I. Introduction

Electrolyte solutions play an important role in many atmospheric and biological systems. Elucidating the chemistry at the surface of aqueous inorganic acid and salt solutions advances understanding of processes such as heterogeneous cloud nucleation[1,2] and ionic transport across membranes.[3,4] A relevant and much debated question is: How does the presence of ions in solution affect the structure of water at the air−liquid interface? Using sum frequency generation (SFG), we find that 0.01*x* and 0.1*x* (x = mole fraction) NaCl do not affect surface water molecules; the spectra resemble that of the neat water surface. However, adding 0.01*x* $KHSO_4$ or 0.2*x* $NaNO_3$ disrupts the first layer of surface water molecules, and 0.01*x* acid solutions have an even more dramatic effect on interfacial water—these ions approach nearer to the first layer.

In this study, the influence of subsurface ions on the structure of surface water is examined for solutions of NaCl, HCl, $NaNO_3$, HNO_3, $KHSO_4$, and H_2SO_4 using the nonlinear spectroscopic technique, SFG. SFG is ideal for this application because of its high sensitivity to the interface at which inversion symmetry is broken. Acids and salts with common anions are chosen to determine the effect of cations versus protons on the structure of interfacial water. All three acids strongly order hydrogen-bonded surface water molecules. In 0.01*x* acid solutions, the significant increase of the hydrogen-bonded water intensity and the decrease of dangling O−H groups indicate that there is significant electrostatic perturbation of the water structure. In comparison, for 0.01*x* salt solutions, the essentially undisturbed hydrogen-bonded region indicates that the electrostatic perturbation is greatly diminished and that the hydration shells of salt complexes displace the dangling O−H bonds.

As discussed below, resonant SFG intensity is enhanced by increased alignment of H_2O molecules with the surface normal and a net increase in the number of oriented molecules. Several interpretations have been proposed to account for the increased intensity of hydrogen-bonded water in 0.01*x* acidic solutions. For example, results from an SFG experiment on the surface of H_2O/H_2SO_4 solutions have been interpreted to describe surface water molecules as tetrahedrally ordered, resembling an icelike structure due to more local order induced by H_2SO_4.[5] Another interpretation of increased SFG intensity of hydrogen-bonded water, based in part on the work of Okumura and co-workers[6] and Johnson and co-workers,[7] is that direct bonding of surface water molecules to anions results in increased SFG signal.

Alternatively, the enhancement of SFG signal is explained by an electric double layer model.[8−11] As described in the Discussion, an electric double layer forms in electrolyte solutions as a result of anions approaching closer to the vapor−liquid interface than cations.[12−14] In this model, the increased SFG intensity results from surface water molecules responding to a subsurface electric field. This model is favored because it explains the enhanced SFG signal in *all* of the acid solutions, 0.01*x* HCl, HNO_3, and H_2SO_4. Also, it accounts for the lack of frequency shift that would accompany direct bonding of water molecules to anions.

SFG theory has been described previously;[15−19] therefore, only a brief description is given here. SFG results from the spatial and temporal overlap of two laser beams at the surface. If one is a visible and the other a tunable infrared beam, an enhancement of SFG signal occurs when the frequency of the infrared light is in resonance with a vibrational transition. On the molecular level, the microscopic hyperpolarizability, $\beta^{(2)}$, is related to the product of the Raman polarizability tensor component, α, and the infrared transition dipole moment, μ:[16]

$$\beta^{(2)} = \langle g|\alpha|\nu\rangle\langle\nu|\mu|g\rangle \quad (1)$$

where ν and g are the excited and ground vibrational states, respectively. Therefore, the vibration must be both Raman and infrared active to produce an SFG signal.

* To whom correspondence should be addressed. E-mail: mshultz1@emerald.tufts.edu

†Department of Chemistry, University of California, Berkeley, California 94720

10.1021/jp992223l CCC: $19.00
Published on Web 12/22/1999

The magnitude of $\chi^{(2)}$, the macroscopic, nonlinear susceptibility, is related to $\beta^{(2)}$ and the number of molecules, N, contributing to the signal:

$$\chi^{(2)} = N\langle\beta^{(2)}\rangle \quad (2)$$

where $\langle ... \rangle$ denotes the orientational average. The SFG signal is proportional to the induced polarization, P_{SI}, which is related to the macroscopic susceptibility tensor

$$I_{SFG} \propto$$

$$|\mathbf{P}_{SI}|^2 = [\Sigma_{J,K}\chi^{(2)}_{IJK}(\mathbf{E}_J(\omega_1)\mathbf{E}_K(\omega_2) + \mathbf{E}_J(\omega_2)\mathbf{E}_K(\omega_1))]^2 \quad (3)$$

where $\mathbf{E}_J$ and $\mathbf{E}_K$ are the incident infrared and visible light fields, respectively, and I, J, and K are the Cartesian coordinates in the laboratory frame. The first term in parentheses contains the resonant contribution, whereas the second contributes to the nonresonant signal background, which is negligible for aqueous solutions.[16,19]

II. Experimental Section

The experimental setup has been detailed previously.[8,10,20] The visible and infrared beams are generated by a LaserVision KTP-based OPO/OPA, pumped by a Spectra-Physics nanosecond GCR-150 YAG laser. The infrared light is tunable from 2500 to 4000 cm^{-1} with an energy of 0.4−5.0 mJ/pulse and a 4 cm^{-1} bandwidth. The copropagating 532 nm and infrared beams impinge on the surface at 52° and 46°, respectively, to produce SFG at 51° from the surface normal. The 532 nm energy density is 400 mJ/cm^2, and the infrared energy density is 100 mJ/cm^2. The SFG signal is selected with a Jarrell-Ash 0.25 m monochromator and detected with a Hamamatsu R3443 photomultiplier tube, a gated boxcar averager, and a computer.

The beam polarizations are *s*-SFG, *s*-visible, and *p*-infrared. Spectra are normalized to the infrared beam intensity at each point and referenced to the free-OH peak intensity of neat water. Three or four spectra at 400 shots per data point are averaged to produce the presented spectra with 1σ standard deviation error bars. The temperature was maintained at 277 K in an ice−water bath. Samples were prepared with reagents from GFS Chemicals and 18 MΩ·cm water from a Barnstead/Thermolyne NANOpure Infinity UV. The insoluble particulates in some saturated salt solutions were filtered with a Whatman PVDF, sterile 0.2 μm Luer Lok syringe filter system. The sodium nitrate solution was prepared by combining HNO_3 and NaOH until neutral pH resulted. Organic impurities in the solutions were below the SFG detection limit (0.05 monolayer).

III. Results

The SFG spectrum of neat water (Figure 1) contains hydrogen-bonded vibrational modes between 3000 and 3600 cm^{-1} and the free-OH peak at 3700 cm^{-1}. At this higher resolution, the SFG water spectrum is consistent with those presented earlier.[21] The free-OH peak corresponds to dangling O−H groups projecting out of the bulk solution into the vapor phase, free of hydrogen bonding. Although the assignment of the hydrogen-bonded peaks is controversial, the interpretation adopted by us and others is based on infrared and Raman experiments of aqueous solutions and ice.[22−25] The peak at ~3150 cm^{-1} is used as an indicator of ordered, tetrahedrally structured H_2O molecules and is assigned to the symmetric stretch of hydrogen-bonded water in a symmetrical environment.[23,25] The peak at ~3400 cm^{-1} is a convolution of at least two resonances: the OH stretch of water in an asymmetrical environment and the antisymmetric stretch of water in a symmetrical environment.[22−28] The 3700 and 3150 cm^{-1} peaks are the focus of this discussion.

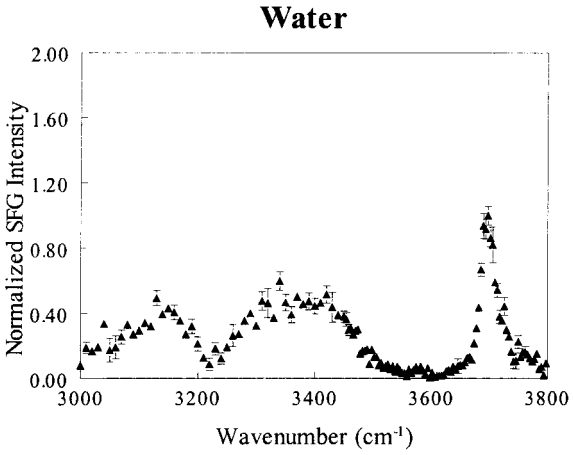

Figure 1. SFG spectrum of neat, liquid water. The polarization is *ssp* and the temperature is 277 K. The spectrum is referenced to the free-OH peak intensity at 3700 cm^{-1}.

The contrast between 0.01*x* acid solutions and 0.01*x* salt solutions is shown in Figures 2 and 3. Parts A and B of Figure 3 summarize the SFG data as: (A) the average maximum intensity in the 3130−3170 cm^{-1} region and (B) the integral of the 3700 cm^{-1} peak. The most striking feature is the 4-fold increase in the 3150 cm^{-1} peak intensity for 0.01*x* H_2SO_4 compared to pure water. Although it remains prominent, this peak intensity decreases in the order H_2SO_4 > HCl > HNO_3 for 0.01*x* acid solutions, as shown in Figure 3A. The free-OH resonance at 3700 cm^{-1} has a slightly different order: HCl > H_2SO_4 > HNO_3 for 0.01*x* acid solutions (Figure 3B).

The SFG spectra and relative peak intensities for 0.01*x* salts, that is, NaCl, $NaNO_3$, and $KHSO_4$, are given in Figures 2 and 3. Potassium and sodium ions may be compared directly because their similar charge density results in comparable electrostatic interactions with ions and water.[29] The hydrogen-bonded region of 0.01*x* NaCl, $NaNO_3$, and $KHSO_4$ solutions are of comparable intensity to that of the neat-water spectrum; that is, the intensity between 3000 and 3600 cm^{-1} is nearly independent of anion. In contrast, the intensity of the free-OH peak (Figures 2 and 3B) is dependent on the anion. The peaks for 0.01*x* NaCl and $NaNO_3$ are about 75% of the intensity for water, whereas the peak for 0.01*x* $KHSO_4$ is only half as intense as water.

The correlation between free-OH peak intensity and anion size was expanded to higher concentrations. The dangling-OH groups are only slightly perturbed for 0.01*x* NaCl and $NaNO_3$ solutions. Increasing the concentration to saturation, the free-OH peak for 0.01*x* NaCl (spectrum not shown) remains only slightly diminished. The SFG intensity for saturated 0.2*x* $NaNO_3$ (Figure 4) solution, however, is about half that of the free-OH peak intensity for water. Thus, the more concentrated 0.2*x* NO_3^- solution and the lower concentration solution with the larger anion (0.01*x* HSO_4^-) affect dangling O−H groups similarly.

IV. Discussion

Bulk-Phase, Surface Studies, and SFG. Numerous investigations of bulk ionic solutions have been conducted. For example, Raman spectroscopy reveals that ions in solution dramatically affect the shape and intensity of the hydrogen-bonded water band.[30−33] NMR studies investigate resonances

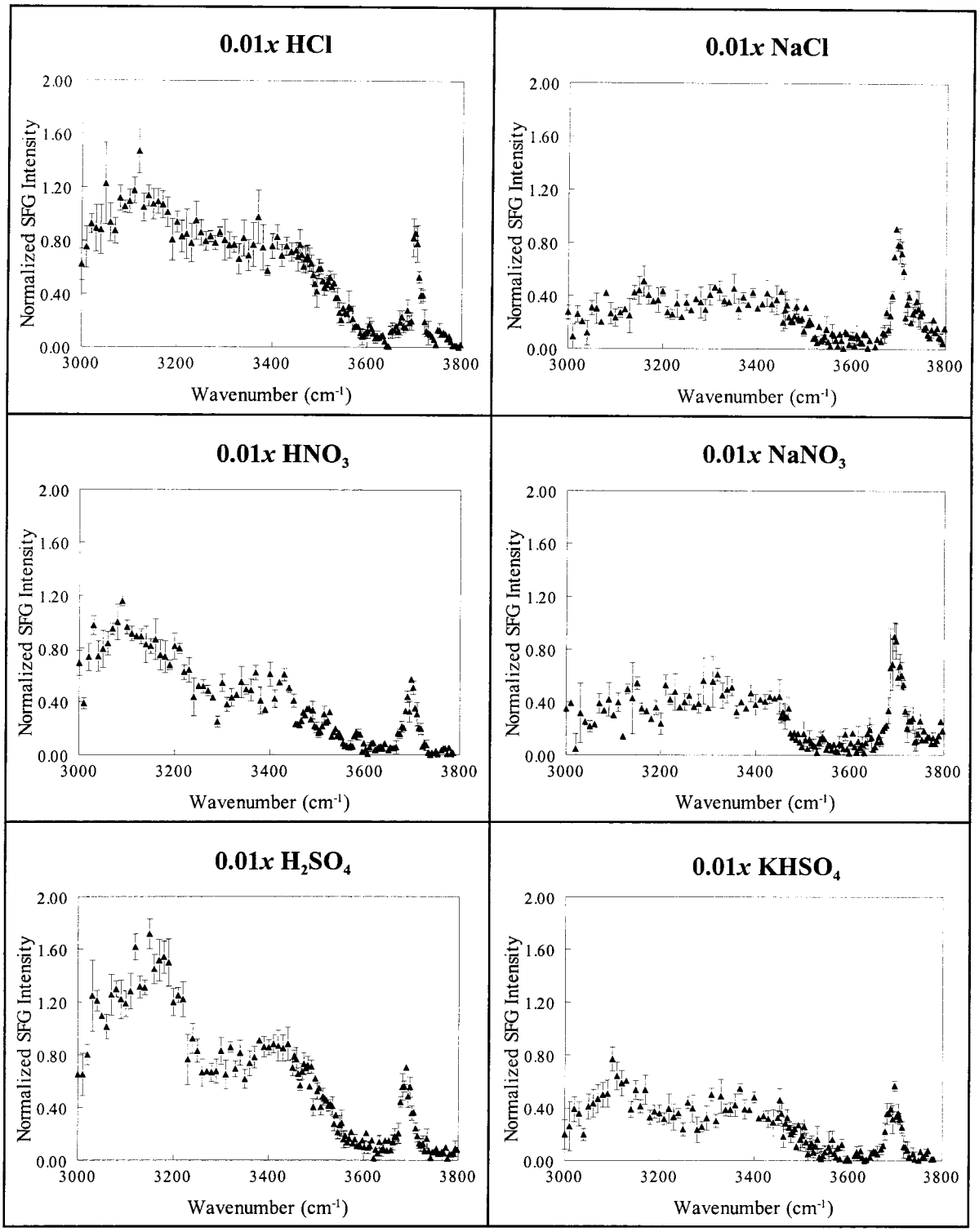

Figure 2. SFG spectra of 0.01 mole fraction solutions at the air−solution interface. The polarization is *ssp*, and the temperature is 277 K. The spectra are referenced to the SFG free-OH peak intensity of neat water.

from nuclei present in the ions to give information about ion−solvent and ion−ion interactions.[29,34,35] However, it is difficult to deduce the structure at the surface from these bulk studies because anions and cations in the bulk are uniformly distributed, and water molecules are subjected to an essentially symmetric force field. In contrast, the surface features an asymmetric field and concentration gradients.

Traditionally, the surfaces of electrolyte solutions have been examined with surface potential[14,36] and surface tension measurements.[37−40] Those techniques probe the surface on a micron-size scale. For SFG, the probe depth is limited by the coherence length − tens of nanometers. Within this length, due to the averaging indicated in eq 2, only net oriented molecules contribute to the signal. The result is a sensitivity to the first layer of solution and the immediate subsurface, referred to as the surface zone. The 3700 cm^{-1} peak necessarily originates from the first layer of water molecules; hydrogen bonding inherent in subsequent layers, red shifts this resonance significantly. The hydrogen-bonded peaks provide information on oriented molecules within the entire surface zone.

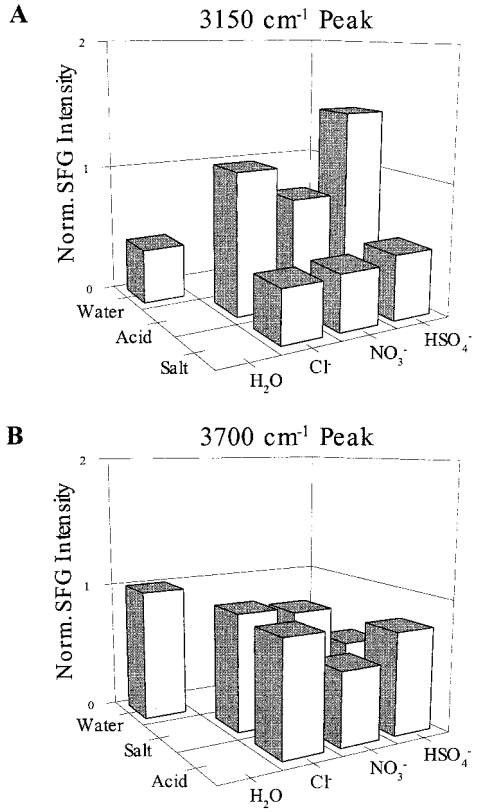

Figure 3. SFG intensity for water and 0.01*x* acids and salts: (A) 3150 cm^{-1} (B) 3700 cm^{-1}. Note the ordering of water, acid, salt in (A) is different than that of water, salt, acid in (B).

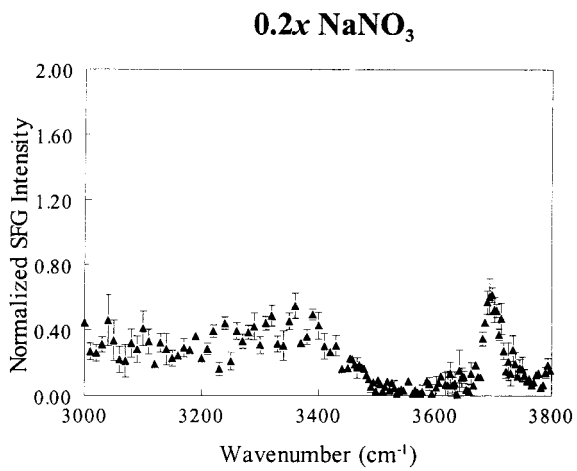

Figure 4. SFG spectrum of 0.2 mole fraction $NaNO_3$ solution at the air−solution interface. The polarization is *ssp*, and the temperature is 277 K. The spectrum is referenced to the SFG free-OH peak intensity of neat water.

As indicated in eqs 2 and 3, SFG intensity is enhanced either by (i) a larger number of oriented molecules or (ii) an increased alignment of the dipole along the surface normal. The number of molecules (i) affects the signal because the SFG intensity is proportional to the square of the number of molecules contributing to the signal (*N*). Molecules with a net orientation within the coherence length contribute to the signal. Therefore, SFG signal increases, for example, as more layers of molecules respond to an electric field. Increased alignment (ii) enhances the signal because a more vertical average orientation results in a larger projection of the molecular dipole onto the surface normal. The $\langle\beta^{(2)}\rangle$ of eq 2 contains the projection information. Equation 3 indicates that the signal grows with the square of this projection. Hence, enhanced SFG signal indicates a convolution of more layers of ordered molecules (i) and greater alignment of their dipoles with the surface normal (ii).

The Electric Double Layer. Previous SFG studies support the existence of an electric double layer consisting of subsurface anions and cations.[8−11] At the air−liquid interface, an electric double layer is defined as the ion distribution in which the larger, more polarizable ions, usually anions, approach the surface more than the less polarizable cations. Evidence of its existence relies on experiments and calculations that have determined a tendency for anions to partition to the surface over cations. For example, a change in surface potential for inorganic ionic solutions, compared to that of pure water, suggests that anions penetrate closer to the interface.[13,14,36] Furthermore, molecular dynamics calculations indicate that the free energy required to move Cl^- and F^- anions to the air−liquid interface is considerably less than that for the Na^+ cation.[12]

For the solutions under consideration, an electric double layer develops near the surface as a result of chloride, nitrate, or bisulfate anions approaching the gas−liquid interface more than protons. Therefore, a gradient exists due to the differential charge distribution with a partial negative charge near the surface. The water molecules in the surface zone respond to the excess negative charge near the surface by pointing their hydrogen atoms into the bulk solution. Consequently, the SFG intensity increases as a greater number of water molecules align with the electric field.

Mechanisms of Surface Perturbation. In a qualitative sense, there are two ways that ionic solutions perturb surface water: electrostatically and by displacement. An electrostatic perturbation refers to the effect of the leading edge of the double layer reaching the first layer of solution; a displacement refers to an associated ion pair or molecular species, such as $H^+ \cdot HSO_4^-$ or H_2SO_4, complexing water in the surface zone. It is suggested that the nature of the solution dictates which mechanism is more significant: electrostatic for 0.01*x acid* solutions and displacement for 0.01*x salt* solutions.

The intense SFG signal in the hydrogen-bonded region for 0.01*x* acid solutions (Figures 2 and 3A) is consistent with ordered water molecules due to the presence of an electric double layer. The subsurface electric field modifies the surface zone of water *including* the free-OH groups because the network is quite extensive[41] and relatively long range.[42] The displacement mechanism is not consistent with the SFG acid solution spectra because the presence of contact ion pairs in the surface zone would collapse the electric double layer, thereby diminishing the 3150 cm^{-1} peak intensity. Indeed, this collapse occurs when acid concentration is increased.[8,11]

The displacement mechanism refers to a contact ion pair which perturbs the surface zone, distorts the hydrogen-bonded network, and ties up the dangling O−H bonds. In salt solutions, this mechanism dominates because the SFG intensity in the 3150 cm^{-1} region is about the same as that in neat water (Figure 3A), contradicting a strong subsurface electric field. There is precedent for salts forming contact ion pairs at these concentrations from previous studies.[43−45] The hydration shell of contact ion pairs disrupt the hydrogen-bonded network of water molecules. With the negative ion closer to the surface, the dangling hydrogens are tied up. For example, K^+ and HSO_4^- in 0.01*x* $KHSO_4$ form contact ion pairs that sufficiently approach the air−liquid interface to diminish the free-OH peak intensity. Increasing the salt concentration enhances the contact ion pairs and magnifies this effect. For example, a comparison of 0.01*x* and 0.2*x* $NaNO_3$ (Figures 2 and 4) illustrates this diminishment

TABLE 1: Ionic Radii,[51] Enthalpy, and Gibbs Free Energy of Hydration for a Select Group of Ions[46,47,50,52,53]

ion	r (Å) (crystal)	$-\Delta H_h$ (kJ/mol)	$-\Delta G_h$ (kJ/mol)
H^+		1129	1090
Li^+	0.60	559	517
Na^+	0.95	444	411
K^+	1.33	360	338
Cl^-	1.81	340	317
I^-	2.16	268	257

of free-OH groups. In summary, the perturbation of dangling O−H groups on salt solutions is a function of ionic strength, ion association, and anion charge density.

Electrostatic Interactions: Hydrated Cations and the Electric Double Layer. An examination of the spectra in Figures 1 and 2, and the summary plots of Figure 3, reveals the significantly greater SFG intensity of hydrogen-bonded water for acid solutions than for either salt solutions or neat water. This is a result of the unique nature of the hydrated proton and the greater association of Na^+ and K^+ with the anions. The ionic radii, enthalpy, and Gibbs free energy of hydration are listed in Table 1 for a select group of cations and anions. The data illustrate the unique nature of proton hydration compared to that of Li^+, Na^+, or K^+. In general, as the ionic radius increases within the same periodic group, $-\Delta H_h$ and $-\Delta G_h$ decrease.[46−49] A comparison between the enthalpy of hydration for the proton and the other cations is startling: proton hydration is at least twice as large as that of Li^+, Na^+, or K^+. In addition, hydrogen is much less polarizable than the remaining Group IA elements. These large differences indicate the extensive hydration of the proton.[50]

The enthalpy of hydration of H^+ may be used to deduce some of the structure of the hydrated proton and thus provide information about the electric double layer. The proton ΔH_h is commonly accepted as −1129 kJ/mol, and much of this stabilization comes from the addition of the first water molecule.[50] The convention of using H_3O^+ is consistent with this observation, but thought must be given to the arrangement of additional water molecules around H_3O^+. Considering the net positive charge on the hydrogen atoms, it is reasonable to assume that each hydrogen in H_3O^+ is hydrogen-bonded to a water molecule. The calculations support this reasoning and predict that the equilibrium structure stoichiometry is $H_9O_4^+$.[50,54,55] The result of these additional water molecules is less contact between the hydrated proton and the anion compared to the corresponding sodium- or potassium-anion interactions. Thus, water molecules at the surface of acid solutions respond more strongly than the salt solutions to a greater negative charge from the electric double layer because protons are less associated with the anions.

Anion Effects. Within the SFG acid series in Figures 2 and 3, one observes that various concentrations of Cl^-, NO_3^-, and HSO_4^- (SO_4^{2-}) alter the structure of hydrogen-bonded water differently.[8,9,11] The 3150 cm^{-1} peak intensity is greatest for H_2SO_4, closely followed by HCl, and it is the least for HNO_3. Therefore, the mechanism that results in the enhancement of SFG intensity for hydrogen-bonded water follows the trend $H_2SO_4 \geq HCl > HNO_3$. This is interpreted in light of the ion association and the electric double layer model.

The pK_A values of −7.3 for HCl, approximately −6 (first pK_A) for H_2SO_4, and −1.3 for HNO_3 indicate that the acid strengths are comparable for HCl and H_2SO_4 and considerably less for nitric acid.[56] The greater concentration of unassociated protons and anions in HCl and H_2SO_4 solutions results in a more extensive electric double layer than in HNO_3 solutions. The increased peak intensity for HCl and H_2SO_4 solutions (Figure 3A) is greater than the HNO_3 solution, consistent with the interpretation that the 3150 cm^{-1} SFG peak intensity is correlated with acid dissociation values and reflects the extent of the electric double layer.

Comparison of Surface Potential, Surface Tension, and SFG Results. Surface potential and surface tension measurements are the classic techniques to determine the surface zone composition for liquid solutions. SFG measurements help to resolve the apparent contradiction raised by surface tension and surface potential measurements for HNO_3 and HCl. Specifically, surface potential measurements suggest that these are typical strong electrolytes that change the surface potential compared with that of water, but the surface tension decreases indicating that HCl and HNO_3 are in the surface.[13,14] SFG measurements suggest that the surface tension decrease is, at least partially, due to reorientation of water in response to the subsurface ions. Furthermore, the surface potential increase for HNO_3 is approximately double that of HCl, indicating a greater surface concentration of HNO_3 than HCl.[11] This is consistent with the SFG measurements reported earlier, which found that HCl is not present on the surface of any solution save that of neat HCl.[9,57]

V. Conclusion

Sum frequency generation spectra of water at the surface of aqueous inorganic acid and salt solutions are examined. Compared to pure water, 0.01x (x = mole fraction) HCl, HNO_3, and H_2SO_4 solutions affect SFG intensity in the hydrogen-bonded region more than 0.01x NaCl, $NaNO_3$, and $KHSO_4$ solutions. This suggests that surface water molecules in acid solutions have greater alignment with the surface normal than those in the salt solutions, and/or more water layers are oriented. This is interpreted in terms of the electric double layer model, in which subsurface anions are closer to the air−liquid interface than cations. The interfacial region of an acid solution possesses a stronger electric field because the highly hydrated proton is not associated with the anions as much as Na^+ and K^+ ions. In the other vibrational region, 3700 cm^{-1}, decreased free-OH peak intensity is interpreted in terms of two mechanisms: electrostatic interactions in 0.01x acid solutions and displacement of water by contact ion pair complexes that disrupt the hydrogen-bonded region in salt solutions. The SFG results are discussed in terms of surface potential and surface tension observations.

Acknowledgment. A special thanks to Mr. Aaron Badgley and Mr. Mark Mellum from GFS Chemicals for preparing solutions to the desired specifications and to Ms. Colleen Bleczinski for helpful suggestions about filtration. Partial support of this work is provided from the US Environmental Protection Agency (Award No. R-822453-01-0).

References and Notes

(1) Gong, S. L.; Barrie, L. A.; Blanchet, L.-P. *J. Geophys. Res.* **1997**, *102*, 3805−3818.

(2) Vogt, R.; Finlayson-Pitts, B. J. *J. Phys. Chem.* **1995**, *99*, 17269−17272.

(3) McLaughlin, S. In *Annu. Rev. Biophys. Chem.*; Engelman, D. M., Ed.; Annual Reviews Inc.: Palo Alto, 1989; Vol. 18, pp 113−136.

(4) Honig, B. H.; Hubbell, W. L.; Flewelling, R. R. In *Annu. Rev. Biophys. Chem.*; Engelman, D. M., Ed.; Annual Reviews Inc.: Palo Alto, 1986; Vol. 15, pp 163−193.

(5) Raduge, C.; Pflumio, V.; Shen, Y. R. *Chem. Phys. Lett.* **1997**, *274*, 140−144.

(6) Choi, J.-H.; Kuwata, K. T.; Cao, Y.-B.; Okumura, M. *J. Phys. Chem. A* **1998**, *102*, 509−507.

(7) Ayotte, P.; Weddle, G. H.; Kim, J.; Johnson, M. A. *J. Am. Chem. Soc.* **1998**, *120*, 12361−12362.
(8) Baldelli, S.; Schnitzer, C.; Shultz, M. J.; Campbell, D. J. *J. Phys. Chem. B* **1997**, *101*, 10435−10441.
(9) Baldelli, S.; Schnitzer, C.; Shultz, M. J. *Chem. Phys. Lett.* **1999**, *302*, 157−163.
(10) Baldelli, S.; Schnitzer, C.; Campbell, D. J.; Shultz, M. J. *J. Phys. Chem. B* **1999**, *103*, 2789−2795.
(11) Schnitzer, C.; Baldelli, S.; Campbell, D. J.; Shultz, M. J. *J. Phys. Chem. A* **1999**, *103*, 6383−6386.
(12) Wilson, M. A.; Pohorille, A. *J. Chem. Phys.* **1991**, *95*, 6005−6013.
(13) Randles, J. E. B. *Phys. Chem. Liq.* **1977**, *7*, 107−179.
(14) Jarvis, N. L.; Scheiman, M. A. *J. Phys. Chem.* **1968**, *72*, 74−78.
(15) Zhu, X. D.; Suhr, H.; Shen, Y. R. *Phys. Rev. B* **1987**, *35*, 3047−3050.
(16) Shen, Y. R. *The Principles of Nonlinear Optics*; John Wiley & Sons: New York, 1984.
(17) Guyot-Sionnest, P.; Superfine, R.; Hunt, J. H.; Shen, Y. R. *Chem. Phys. Lett.* **1988**, *144*, 1−5.
(18) Bain, C. D. *J. Chem. Soc., Faraday Trans.* **1995**, *91*, 1281−1296.
(19) Hirose, C.; Akamatsu, N.; Domen, K. *J. Chem. Phys.* **1992**, *96*, 997−1004.
(20) Baldelli, S.; Schnitzer, C.; Shultz, M. J.; Campbell, D. J. *J. Phys. Chem. B* **1997**, *101*, 4607−4612.
(21) Du, Q.; Superfine, R.; Freysz, E.; Shen, Y. R. *Phys. Rev. Lett.* **1993**, *70*, 2313−2316.
(22) Scherer, J. R. In *Advances in Infrared and Raman Spectroscopy*; Clark, R. J. H., Hester, R. E., Eds.; Heyden: Philadelphia, 1978; Vol. 5, pp 149−216.
(23) Scherer, J. R.; Go, M. K.; Kint, S. *J. Phys. Chem.* **1974**, *78*, 1304−1313.
(24) Irish, D. E.; Brooker, M. H. In *Advances in Infrared and Raman Spectroscopy*; Clark, R. J. H., Hester, R. E., Eds.; Heyden & Sons: London, 1981; Vol. 2, pp 212−311.
(25) Brooker, M. H.; Hancock, G.; Rice, B. C.; Shapter, J. *J. Raman Spectrosc.* **1989**, *20*, 683−694.
(26) Bertie, J. E.; Whalley, E. *J. Chem. Phys.* **1964**, *40*, 1637−1644.
(27) Cunningham, K.; Lyons, P. A. *J. Chem. Phys.* **1973**, *59*, 2132−2139.
(28) Ayers, G. P.; Pullin, A. D. E. *Chem. Phys. Lett.* **1974**, *29*, 609−615.
(29) Deverell, C.; Richards, R. E. *Mol. Phys.* **1969**, *16*, 421−439.
(30) Lauwers, H. A.; Kelen, G. P. V. d. *Bull. Soc. Chim. Belg.* **1963**, *72*, 477−499.
(31) Terpestra, P.; Combes, D.; Zwick, A. *J. Chem. Phys.* **1990**, *92*, 65−70.
(32) Bekkiev, A. Y.; Fadeev, V. V. *Sov. Phys. Dokl.* **1982**, *27*, 63−64.
(33) Gogolinskaya, T. A.; Patsaeva, S. V.; Fadeev, V. V. *Sov. Phys. Dokl.* **1986**, *31*, 820−822.
(34) Akitt, J. W. *J. Chem. Soc., Dalton Trans.* **1973**, *1*, 49−52.
(35) Deverell, C.; Richards, R. E. *Mol. Phys.* **1966**, *10*, 551−564.
(36) Randles, J. E. B. In *Discuss. Faraday Soc.*; The Aberdeen University Press Ltd.: Aberdeen, 1957; Vol. 24, pp 194−199.
(37) Chattoraj, D. K.; Moulik, S. P. In *Adsorption at Interfaces*; Mittal, K. L., Ed.; American Chemical Society: Washington, D. C., 1975; pp 48−62.
(38) Onsager, L.; Samaras, N. N. T. *J. Chem. Phys.* **1934**, *2*, 528.
(39) Hard, S.; Johansson, K. *J. Colloid Interface Sci.* **1977**, *60*, 467−472.
(40) Harkins, W. D.; McLaughlin, H. M. *J. Am. Chem. Soc.* **1925**, *47*, 2083−2089.
(41) Stanley, H. E.; Teixeira, J. *J. Chem. Phys.* **1980**, *73*, 3404−3422.
(42) Israelachvili, J. N. In *The Handbook of Surface Imaging and Visualization*; Hubbard, A. T., Ed.; CRC Press: Boca Raton, 1995.
(43) Fleissner, G.; Hallbrucker, A.; Mayer, E. *J. Chem. Soc., Faraday Trans.* **1996**, *92*, 23−28.
(44) Irish, D. E.; Davis, A. R. *Can. J. Chem.* **1968**, *46*, 943−951.
(45) Rull, F. *Z. Naturforsch.* **1995**, *50a*, 292−300.
(46) Dzidic, I.; Kebarle, P. *J. Phys. Chem.* **1970**, *74*, 1466−1474.
(47) Arshadi, M.; Yamdagni, R.; Kebarle, P. *J. Phys. Chem.* **1970**, *74*, 1475−1482.
(48) Randles, J. E. B. *Trans. Faraday Soc.* **1956**, *52*, 1573−1581.
(49) Stokes, R. H.; Robinson, R. A. *J. Am. Chem. Soc.* **1948**, *70*, 1870−1878.
(50) Murrell, J. N.; Jenkins, A. D. *Properties of Liquids and Solutions*, 2nd ed.; John Wiley and Sons: Chichester, 1994.
(51) Pauling, L. *The Nature of the Chemical Bond and the Structure of Molecules and Crystals*, 3rd ed.; Cornell University Press: Ithaca, NY, 1960.
(52) Hepler, L. G.; Woolley, E. M. In *Water, A Comprehensive Treatise*; Franks, F., Ed.; Plenum Press: New York, 1973; Vol. 3, pp 145−172.
(53) Kebarle, P.; Searles, S. K.; Zolla, A.; Scarborough, J.; Arshardi, M. *J. Am. Chem. Soc.* **1967**, *89*, 6393.
(54) Beckey, H. D. *Z. Naturforsch.* **1959**, *14a*, 712−721.
(55) Tuck, D. G.; Diamond, R. M. *Proc. Chem. Soc.* **1958**, 236−237.
(56) Perrin, D. D. *Ionisation Constants of Inorganic Acids and Bases in Aqueous Solution*, 2nd ed.; Pergamon Press: New York, 1982.
(57) Baldelli, S.; Schnitzer, C.; Shultz, M. J. *J. Chem. Phys.* **1998**, *108*, 9817−9820.